Journla of Molecular Pharmaceutics & Organic Process Research

ISSN: 2329-9053

Zhang, J Mol Pharm Org Process Res 2013, 1:1
DOI: 10.4172/2329-9029.1000102

Research Article Open Access

Protective Effects of Acetyl L-Carnitine on Inhalation Anesthetic-Induced Neuronal Damage in the Nonhuman Primate

Zhang X[1], Liu S[1], Paule MG[1], Newport GD[1], Callicott R[1], Berridge MS[2], Apana SM[2], Slikker W Jr[1] and Wang C[1]*

[1]National Center for Toxicological Research, U.S. Food and Drug AdministrationJefferson, Arkansas 72079, USA
[2]3D Imaging, LLC, Little Rock, AR 72113 and University of Arkansas for Medical Sciences, Little Rock, AR 72205, USA

Abstract

The inhalation anesthetics nitrous oxide (N_2O) and isoflurane (ISO) are commonly used for general anesthesia in human infants. Combined exposures to N_2O and ISO are known to cause abnormal apoptotic cell death (neurotoxicity) in pediatric animal models. Acetyl-L-carnitine (ALC), an anti-oxidant dietary supplement, has been reported to minimize neuronal damage in some models of neurotoxicity. MicroPET/CT imaging is capable of detecting and localizing changes in cellular markers of brain damage associated with developmental exposures to general anesthetics. By monitoring changes in glial activation, thought to be a marker of neuroinflammation, it should be possible to determine the intensity, duration and location of neuronal damage associated with exposure to general anesthetics. Here we assessed the uptake of ^{18}F-labeled fluoroethoxybenzyl-N-(4-phenoxypyridin-3-yl) acetamide (FEPPA), a ligand for peripheral benzodiazepine receptors on activated glial cells. On postnatal day (PND) 5, rhesus monkeys (4/group) were exposed to a mixture of 70% N_2O, 29% oxygen plus 1% ISO, or ALC (100 mg/kg given i.p.) plus this mixture for 8 hours; control monkeys with and without ALC were exposed to room air only. [^{18}F]-FEPPA was injected intravenously and microPET/CT images were obtained one day and one and three weeks after anesthetic exposure. One day after anesthetic exposure the uptake of FEPPA was significantly increased only in the temporal lobe and one week after exposure uptake was significantly increased in only the frontal lobe. No significant differences in uptake were seen in any area after 3 weeks. Co-administration of ALC effectively blocked the increase in FEPPA uptake in both the temporal and frontal lobes. These findings suggest that microPET/CT imaging of FEPPA uptake may be useful for monitoring the time-course and location of adverse neural events that are associated with developmental exposures to general anesthetics. In addition, ALC appears to be capable of protecting against at least some of the adverse effects associated with such exposures.

Keywords: Neuronal damage; Acetyl-L-carnitine; Isoflurane

Introduction

Translational molecular imaging using positron emission tomography (PET) is a radionuclide imaging modality that enables direct *in vivo* measurements of multiple biological processes, disease progression and response to therapy in various organs. The development of microPET imaging applications has provided the ability to collect sensitive and quantitative three-dimensional molecular information from the living brains of a variety of animals including nonhuman primates (NHPs) [1-3]. Repeat studies with microPET imaging allow the adverse effects of toxic insults to be followed over time in individual animals that can also serve as their own controls [4-6]. For assessing the neurotoxic effects associated with developmental exposures to anesthesia, we have developed a microPET protocol to target neuronal damage *in vivo* using imaging approaches [7,8].

Exposure to general anesthetics during the period of rapid neuronal growth and synaptogenesis (the brain growth spurt period) in the developing animal brain can induce adverse effects including long-term neurotoxicity and undesired neurological consequence [9-13]. Nonhuman primates are exceptionally good animal models of neurodevelopment and for the detection of potential neurodegenerative effects associated with exposure to inhaled anesthetics. In our previous study [14], neonatal rhesus monkeys (PND 5 or 6) were exposed to a combination of 70% N_2O + 1% ISO to achieve and maintain a surgical plane of anesthesia. Significantly elevated neuronal damage, as indicated by increased numbers of caspase-3-, silver stain-, and Fluoro-Jade C-positive cells, was observed in neocortical areas, especially in layers II and III of the frontal cortex, temporal gyrus and hippocampus. MicroPET scans using [^{18}F]-radiolabelled]-N-(2-(2-fluoroethoxy) benzyl)-N-(4-phenoxypyridin-3-yl) acetamide) ([^{18}F]-FEPPA) (6) demonstrated that anesthetic exposure induced significantly increased uptake of [^{18}F]-FEPPA in the temporal lobe and frontal lobe of exposed animals in time dependent manner.

Acetyl-L-carnitine (ALC) (Figure 1a), an esterified compound of L-carnitine (4-N-trimethylamino-3-hydroxybutyric acid, LC) (Figure 1b), is essential for the β-oxidation of long chain fatty acids in mitochondria to generate ATP. Compared to LC, ALC is more actively transported across the blood-brain barrier and, thus, can be more effective in modulating brain metabolism [15-18]. It has been reported that ALC provides neuroprotective benefits in neurodegenerative and aging situations [19-26], although the mechanism of its neuroprotective effect is not known. The purpose of the current imaging study was to determine if co-administration of ALC could protect or reverse anesthetic-induced neurotoxicity.

Materials and Methods

Animals

All animal procedures were approved by the National Center for

***Corresponding author:** Cheng Wang, Division of Neurotoxicology, National Center for Toxicological Research/FDA, 3900 NCTR Road, Jefferson, AR 72079-9502, USA, Tel: 870-543-7259; Fax: 870-543-7745; E-mail: Cheng.Wang@fda.hhs.gov

Received January 18, 2013; **Accepted** February 26, 2013; **Published** February 28, 2013

Citation: Zhang X, Liu S, Paule MG, Newport GD, Callicott R, et al. (2013) Protective Effects of Acetyl L-Carnitine on Inhalation Anesthetic-Induced Neuronal Damage in the Nonhuman Primate. J Mol Pharm Org Process Res 1: 102. doi:10.4172/2329-9029.1000102

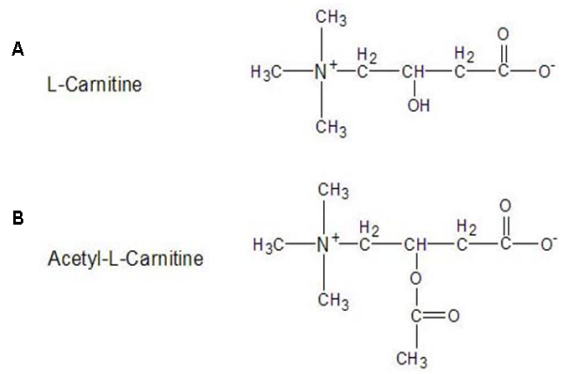

Figure 1: Chemical structure of L-carnitine (LC) and Acetyl-L-carnitine (ALC).

Toxicological Research (NCTR) Institutional Animal Care and Use Committee and conducted in full accordance with the PHS Policy on Humane Care and Use of Laboratory Animals.

All monkeys were born and housed at the FDA's National Center for Toxicological Research nonhuman primate research facility. Animal procedures were designed to minimize the number of animals required and any pain or distress associated with the experimental procedures.

A total of sixteen (PND 5 or 6, 460-500 g) rhesus monkeys (*Macacamulatta*) were utilized. Seven male and nine female monkeys were randomly assigned to control (n=4, 2 males, 2 females), control+ALC (n=4, 2 males, 2 females), ISO+N_2O (n=4, 1 male, 3 females) and ISO+N_2O+aLc (n=4, 2 males, 2 females) groups. Immediately prior to the initiation of anesthesia or sequestration (controls), the neonates were separated from their anesthetized mothers, removed from their home cage and hand carried to a procedure room. Control animals were maintained in a holding cage other than the exposure chamber with water, but no food, and were not sedated for physiological measurements or blood sample collections. Animals in the anesthetic exposure groups were exposed to a mixture of 70% N_2O/29% oxygen and 1% ISO for 8 hours.

Experimental procedures

Nitrous oxide (N_2O) and oxygen were delivered using a calibrated anesthetic machine with blender (Bird Corporation, Palm Springs, CA, USA). Isoflurane (ISO) was delivered using an agent-specific vaporizer (E-Z Anesthesia, Palmer, PA, USA) attached to the anesthetic machine. To administer a specific concentration of N_2O/oxygen/ISO in a tightly controlled environment, an anesthesia chamber (Euthanex Corp. Palmer, PA) was used. Monkeys were kept in this chamber on a circulating water heating pad to maintain body temperature at approximately 37°C throughout the experiment. Stable gas and volatile anesthetic concentrations were attained in the chamber within 5 min of the start of exposure. For controls, room air was used in place of the inhalation anesthetics. For the exposure groups, the N_2O/oxygen/ISO mixture was continuously delivered to the chamber for 8 hours. A relief valve on the anesthesia chamber allowed escape of gases to avoid accumulation of carbon dioxide and waste anesthetic gas was scavenged using an attached canister containing activated charcoal. For groups with ALC, acelyl-l-carnitine (Sigma, St. Louis, MO, USA) was i.p. administered at doses of 100 mg/kg in a saline vehicle, 1 hour before and 4 hours following the start of exposure to room air or the anesthetics.

During the experimental period, dextrose (5%) was administered by stomach tube (5 ml) every 2 h to both treated and control monkeys to maintain blood glucose levels. Glycopyrrolate (0.01 mg/kg, American Reagent, Shirley, NY, USA) was administered intramuscularly prior to exposures to both treated and control monkeys to reduce airway secretions. Once exposures were complete, animals were monitored in an incubator until complete recovery and then returned to their mothers (approximately 2 hours after the 8 hour exposures): control animals were kept in the exposure chambers under room air for a total of 10 hours.

Monitoring of physiological parameters: The physiological parameters of the neonatal monkeys were monitored following procedures described previously [27,28]. Briefly, non-invasive pulse oximetry (N-395 Pulse Oximeter, Nellcor, Pleasanton, CA; MouseO_x Plus Vital Sign Monitor, Starr™ Life Sciences, Oakmont, PA), capnography (Tidal Wave Hand-held capnography, Respironics, Murrysville, PA), sphygmomanometry (Critikon Dynamap Vital Signs Monitor, GE Healthcare, Waukesha, WI, USA), and rectal temperature monitoringwere used to verify the physiological status of subjects. Heart and respiration rates, arterial blood O_2 saturation levels, expired CO_2 concentrations, and rectal temperatures, systolic and diastolic blood pressures were recorded every one or two hours in anesthetized and control animals, respectively. Venous blood (approximately 250 µl) was collected at two-hour intervals for measurement of plasma glucose concentrations, venous blood gases, pH, and hematocrits (GEM®Premier™4000, Instrumentation Laboratory, Lexington, MA). Statistical analyses of physiological parameters were performed using Student's *t*-test for comparisons between treated and control groups. One-way analysis of variance was used to evaluate the effect of time under anesthesia on body temperature. The null hypothesis was rejected at a probability level of $P<0.05$.

Radiotracer preparation: [^{18}F]-FEPPA was prepared by 3D-Imaging LLC (Little Rock, AR) according to Wilson et al. [29] from the corresponding to sylate as described therein with minor modifications to the procedure. [^{18}F]-FEPPA was produced in >98% purity at a specific activity EOS of 1.1-3.7 TBq (30-100 Ci)/µmole, as compared to the previously reported value of 11-37 MBq (0.3-1 Ci)/µmole [30]. Specific activity at the time of use was one tenth to two-thirds of the EOS value.

MicroPET: A commercial high resolution small animal PET scanner (Focus 220, Siemens Preclinical Solution, Knoxville, USA) was used to quantitatively acquire images of the monkey brain. The scanner has 96 lutetium oxyortho-silicate detectors and provides a transaxial resolution of 1.35 mm full-width at half-maximum. Data were collected in a 128×128×95 matrix with a pixel width of 0.475 mm and a slice thickness of 0.815 mm.

Computed tomography: Monkeys were also imaged in a newly developed mobile neurological CereTom CT scanner (Neurologica Corps. Danvers, MA, USA). The CT gantry of the CereTom scanner moves while the subject remains externally supported and fixed in space and therefore allows it to be physically connected to the microPET scanner. Exposure settings for each CT scan were 120 kVp, 5 mAs, scan time=120s. Data were collected in a 512×512 matrix with a pixel width of 0.49 mm and a slice thickness of 1.25 mm.

MicroPET/CT image acquisition: The first microPET and CT scans of each monkey brain weretaken on PND 6 or 7, the day following the experimental exposures on PND 5 or 6. Follow-up microPET/CT scans occurred approximately one week (PND 14), three weeks

(PND 30) and 5 months following treatment (at 6 months of age). For collection of the microPET/CT images, animals were positioned on a modified external bed controlled by the microPET unit. The bed replaced the standard microPET bed and allowed for sufficienttravel to move animals through the microPET and CT fields of view (over an axial range of greater than 50 cm). Throughout microPET/CT imaging sessions, monkeys were anesthetized with 1.5% isoflurane gas alone delivered through a custom face mask and an electronic heating pad was used to maintain body temperature at approximately 37°C. For each imaging session [^{18}F]-FEPPA (56 MBq) was injected into the lateral saphenous vein of each animal (anesthetized). Immediately following the injection, a set of serial microPET images was collected to assess the influx of the tracer for 2 hours (24 frames, 5 min each). Micro-computed tomography (microCT) coronal images were obtained immediately after microPET imaging for the purpose of fusing anatomical (CT) with molecular (PET) data. The microCT images were acquired for 2 min and concurrent image reconstruction was achieved using 3D reconstruction software (ASIPro™; Concorde Microsystems, Inc, Knoxville, TN) installed in the CereTom CT controller unit. Once scanning was complete, animals were monitored in an incubator within a shielded isolation area until complete recovery (approximately 2 hours) and then returned to their mothers. Control animals were kept in the exposure chambers under room air for the same amount of time.

Imaging data analysis: Medical image analysis software, ASIPro™ (Concorde Microsystems, Inc, Knoxville, TN) was used for the anatomical/molecular data fusion and statistical analyses. Regions of Interest (ROIs) were outlined and measured using tools provided by ASIPro™. Radioactivity in different brain areas was also quantified using this software. All images were displayed using the same color scale, shown in figure 2. Tracer accumulations in the ROIs in the left frontal and left temporal cortex were converted to SUVs. The SUVs for the ROIs were compared between control and treatment groups at a variety of time points using RM ANOVA. All values are presented as means+S.E.M. A p value of less than 0.05 was considered statistically significant.

Results

Dynamic [^{18}F]-FEPPA uptake in the cerebral cortex of animals exposed to anesthesia on PND 5 or 6

The first microPET scans of the neonatal monkey brains weretaken on PND 6/7 (one day after the exposure). The follow-up microPET scans were repeated for each monkey on PND 14 (~one week after exposure), and at 1 month (~three weeks after exposure) and 6 months of age.

For each microPET scan, images were obtained over 2 hours following the injection of [^{18}F]-FEPPA and Time Activity Curves (TACs) from the frontal and temporal cortices (the most vulnerable brain areas) [12,14] were obtained (Figure 2). Tracer accumulations in the ROIs were converted to SUVs. [^{18}F]-FEPPA was observed in the ROIs in both control and treated animals demonstrating that it was capable of accessing these brain areas. Examples of the first microPET scans (24 hours after exposure) are shown in figure 2 as coronal, axial and sagital images highlighting [^{18}F]-FEPPA brain concentrations in a treated monkey. The accumulation of [^{18}F]-FEPPA was clearly increased in cortical areas such as the temporal lobe, with significant differences being observed at some time points (Figure 4). The uptake of [^{18}F]-FEPPA in the frontal lobe of treated animals was not statistically significantly increased even though the SUVs at most time points were higher than those in controls.

In order to examine whether acetyl-l-carnitine could prevent or lessen the inhalation anesthetic–induced increase in FEPPA uptake

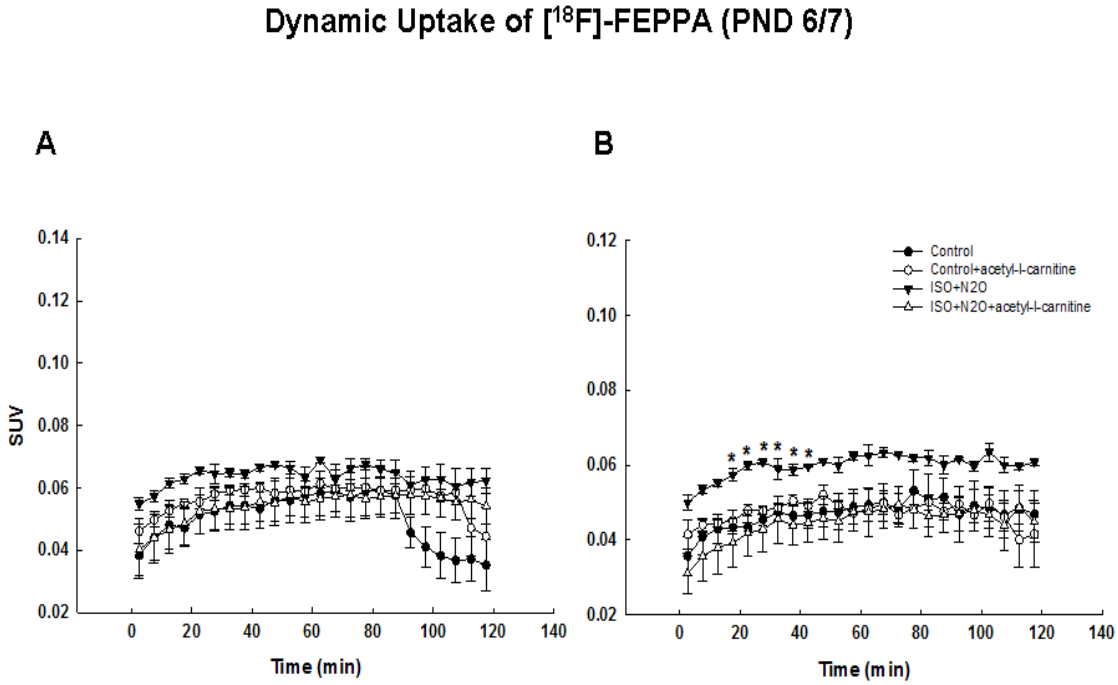

Figure 2: Graph showing the dynamic uptake of ^{18}F-FEPPA expressed as SUV *vs.* time for each ROI (A: left frontal cortex; B: left temporal lobe) from control, control+ALC, anesthetic-treated, anesthetic+ALC treated monkeys on PND 6/7 (n=4/group). SUV=Standard Uptake Value=average concentration of radioactivity in the ROI (MBq/mL) x body weight (gram)/injected dose (MBq). Data are shown as the means ± S.E.M. *p<0.05

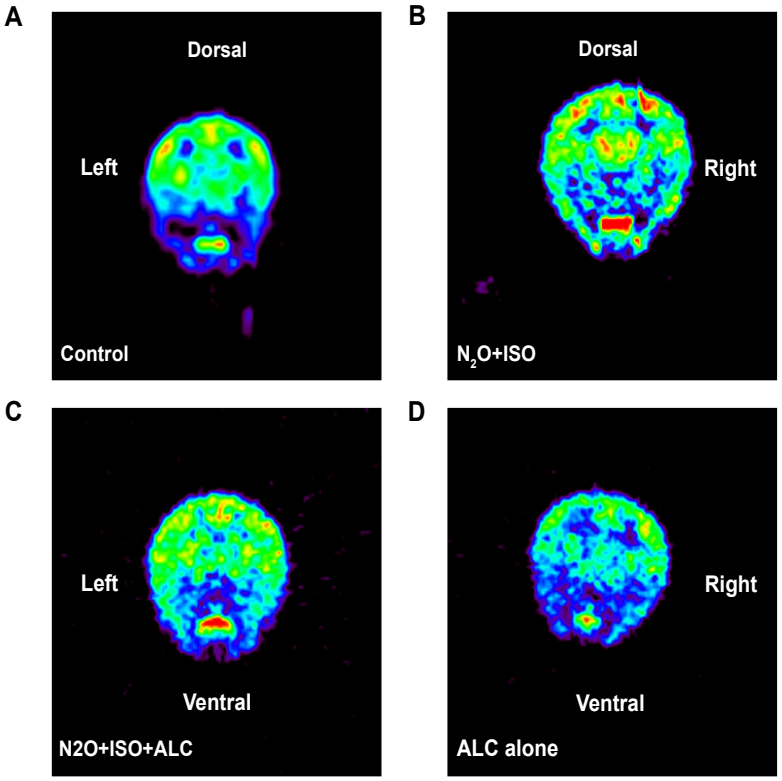

Figure 3: A set of representative microPET images (coronal plane) of a control (A) an anesthetic-treated (B), an anesthetic+ALC (C), and a control+ALC (D) treated monkey brain (B) on PND 14.

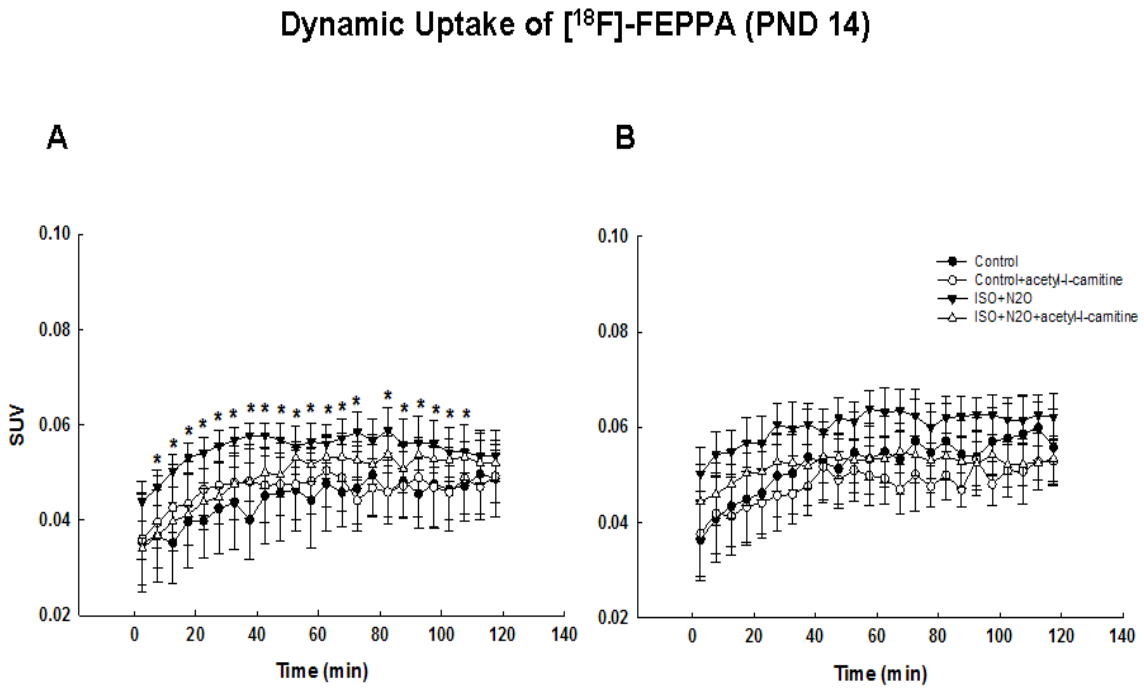

Figure 4: Graph showing the dynamic uptake of ^{18}F-FEPPA expressed as SUV vs. time in the ROI (A: left frontal cortex; B: left temporal lobe) from control, control+ALC, anesthetic-treated, anesthetic+ALC treated monkeys on PND 14 (n=4/group). SUV=Standard Uptake Value=average concentration of radioactivity in the ROI (MBq/mL) × body weight (gram)/injected dose (MBq). Data are shown as the means ± S.E.M. $^{*}p<0.05$

PND 5/6 monkeys were exposed to the anesthetic combination (70% N_2O/30% oxygen and 1% ISO) for 8 h in the presence or absence of acetyl-l-carnitine (100 mg/kg, i.p.). An effect interpreted as protective was evidenced by a significant attenuation of the uptake of radiotracer in the temporal cortex byacetyl-l-carnitine.

Dynamic [^{18}F]-FEPPA uptake in the cerebral cortex on PND 14

On PND14, approximately one week after the anesthetic exposure, SUVs in both the frontal and temporal cortical areas were higher in the exposed animals than in the controls at all time points, demonstrating an increased uptake and retention of [^{18}F]-FEPPA in treated subjects (Figure 3). Statistically significant differences occurred only in the frontal cortical area. Again, ALC treatment resulted in a significant diminution in the uptake of radiotracer in the frontal cortex (Figure 4).

Dynamic [^{18}F]-FEPPA uptake in the cerebral cortex on PND 30 and at 6 months of age

On PND 30, about 3 weeks after anesthetic exposure, the uptake of [^{18}F]-FEPPA in the anesthetic-exposed monkeys was higher than that in the controls at most of the time points, although no significant differences were observed at any time (Figure 5).

At the age of 6 months, the uptake of [^{18}F]-FEPPA in the anesthetic-exposed monkeys was similar to that of controls at most of the time points and no significant differences were observed at any time.

Discussion

Peripheral benzodiazepine receptors (PBR) are mainly located on the outer mitochondrial membrane, the nuclear fractions of normal and cancerous tissue, and in the plasma membrane and membrane of organelles in various cell types [31-34]. In the CNS, PBRs are primarilylocated in glial cells, particularly microglia and astrocytes that participate in multiple physiological functions including neurosteroid synthesis, nutritional support of neurons and modulation of CNS immune reactions [35,36]. The expression of the PBR in brain is significantly increased in response to a wide variety of CNS insults. Following exposure to neurotoxicants and after other forms of neuronal insult, PBR levels increase significantly in both astrocytes and microglia in damaged brain areas in a time-dependent and region-specific fashion. After brain injury, immunolabelling of PBRs has been shown to increase with the increase being localized to mitochondria and other cellular compartments [36-38].

Astrogliosis, an increase in the number of astrocytes generally caused by the destruction of nearby neurons, is considered a universal marker of neurotoxicity/neurodegeneration. Therefore, the PBR is widely recognized as an important target for PET imaging because levels of the PBR increase in areas of insult. Specific ligands for the PBR have been radiolabeled and used in *in vivo* studies in nonhuman primates. Among them, the [^{18}F]-radiolabelled phenoxyanilide, [^{18}F]-FEPPA can be efficiently prepared in high radiochemical yields and at high specific activity. This compound has appropriate lipophilicity for assisting brain penetration and has shown moderate uptake in the rat brain [29,39-41]. Our previous imaging study showed that prolonged exposure to a combination of N_2O and ISO during early development results in neuronal damage in the rhesus monkey [6]. To determine whether injury to brain tissue caused by anesthetic exposure--as evidenced by increases in [^{18}F]-FEPPA uptake--can be ameliorated, the present studies were conducted to assess the efficacy of the putative neuroprotectant, acetyl-L-carnitine.

Acetyl-L-carnitine (ALC), an esterified compound of L-carnitine (LC), is essential for the β-oxidation of long chain fatty acids in mitochondria to generate ATP. As a widely distributed, short-chain ester of LC in the body, ALC is present in relatively high levels in

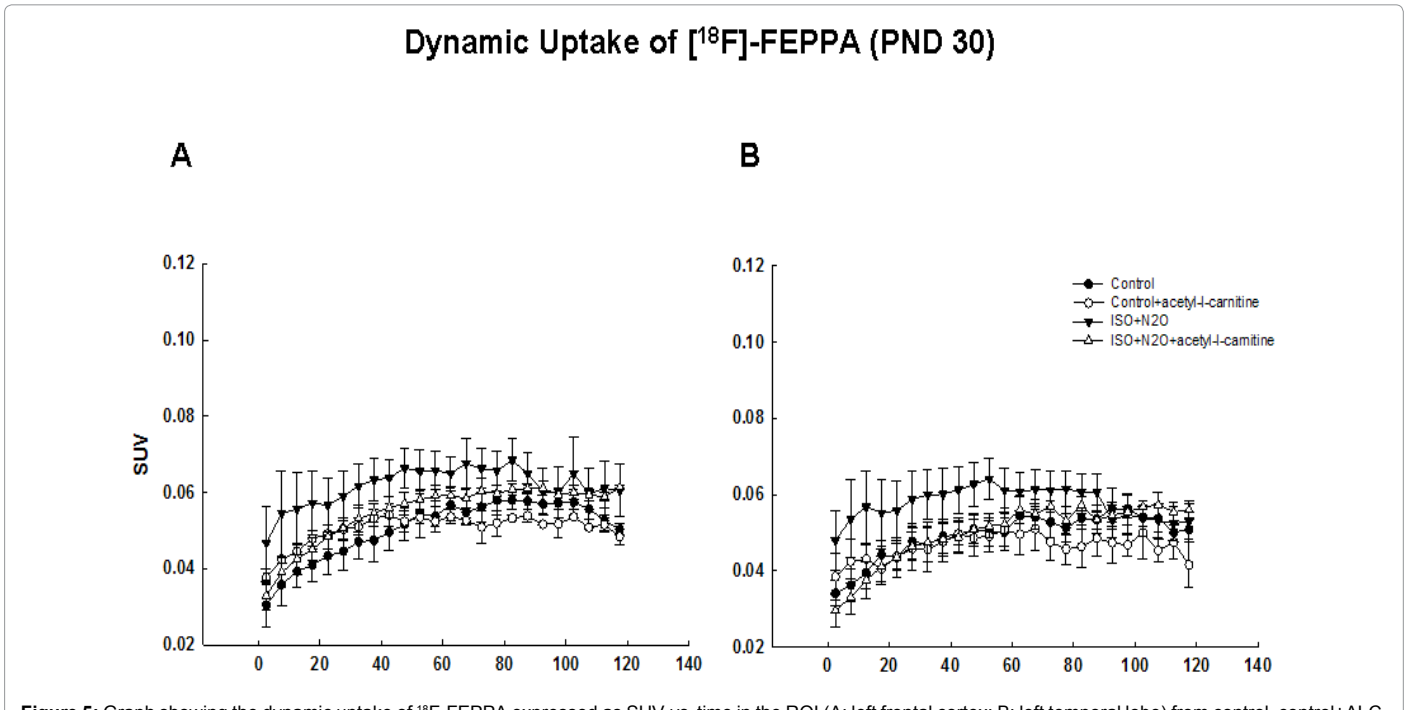

Figure 5: Graph showing the dynamic uptake of ^{18}F-FEPPA expressed as SUV *vs.* time in the ROI (A: left frontal cortex; B: left temporal lobe) from control, control+ALC, anesthetic-treated, anesthetic+ALC treated monkeys on PND 30 (n=4/group). SUV=Standard Uptake Value= average concentration of radioactivity in the ROI (MBq/mL) × body weight (gram)/injected dose (MBq). Data are shown as the means ± S.E.M. $^{*}p<0.05$

the brain where the ratio of ALC to free carnitine is highest [42-45]. Compared to LC, ALC is much more actively transported across the blood-brain barrier and, thus, can more easily affect brain metabolism [15-18]. It has been reported that ALC provides neuroprotective benefits in neurodegenerative diseases and situations of metabolic stress such as ischemia, hypoxia, aging, alcoholism and in traumatic injury [19-26,45-47]. Although the mechanism(s) underlying this neuroprotective effect is not known, it may involve an enhancement of mitochondrial function, its antioxidant activity, it's abiity to stabilize membranes, use energy from the glycolytic pathway, and/or modulate the expression of genes and their proteins that exert anti-oxidant and neurotrophic effects [17,45,48,49]. It has been demonstrated in a variety of *in vitro* and *in vivo* studies that ALC can prevent neuronal death, decrease the loss of dorsal root ganglion cells, enhance the binding of nerve growth factor, and accelerate the regeneration of neurons [45,50,51].

In our previous study [12], brain damage was demonstrated in PND 7 rat pups exposed to N_2O (75%) + ISO (0.55%) with maximal neurodegeneration observed 6–8 h after exposure. This inhaled anesthetic-induced neuronal apoptosis was blocked by the co-administration of LC which was associated with changes in the expression of Bax and BCL-XL. Consistent with these previous experiments, thecurrent study demonstrated that co-treatment of ALC can attenuate the increased uptake of a PBR tracer in cerebral cortex of nonhuman primates exposed to the same inhaled anesthetics. Following such exposures during the brain growth spurt period, it seems that neuronal apoptosis can be initiated by either an intracellular factor, such as increased calcium influx and oxidative stress or by extracellular factors such as inflammatory cytokines. In a lipopolysaccharide-induced systemic inflammation model, ALC significantly decreased levels of TNFα and interleukins and consequently reduced the inflammatory reactions in the brain following acute insult [26,52,53]. This may also partly explain the reason that co-administration of ALC effectively blocked the increase in FEPPA uptake in both the temporal and frontal lobes in the exposed brain of the nonhuman primate.

ALC has been widely used in clinical trials [45] and is considered safe with a very low incidence of significant side effects during long-term administration [54]. Although multiple potential mechanisms of neuroprotection by ALC may be involved--and it is hard to accurately identify the most critical one--it seems appropriate to suggest that ALC be employed as a potential neuroprotective agent to prevent anesthetics-induced brain damage and the development of subsequent long-term neurological deficits.

Acknowledgements

This document has been reviewed in accordance with United States Food and Drug Administration (FDA) policy and approved for publication. Approval does not signify that the contents necessarily reflect the position or opinions of the FDA nor does mention of trade names or commercial products constitute endorsement or recommendation for use. The findings and conclusions in this report are those of the authors and do not necessarily represent the views of the FDA.

This work was supported by the National Center for Toxicological Research (NCTR) (NCTR E-7285)/U.S. Food and Drug Administration (FDA).

References

1. Hillmer AT, Wooten DW, Moirano JM, Slesarev M, Barnhart TE, et al. (2011) Specific α4β2 nicotinic acetylcholine receptor binding of [F-18] nifene in the rhesus monkey. Synapse 65: 1309-1318.
2. Kilbourn MR, Hockley B, Lee L, Sherman P, Quesada C, et al. (2009) Positron emission tomography imaging of (2R,3R)-5-[(18)F]fluoroethoxybenzovesamicol in rat and monkey brain: a radioligand for the vesicular acetylcholine transporter. Nucl Med Biol 36: 489-493.
3. Wooten DW, Moraino JD, Hillmer AT, Engle JW, Dejesus OJ, et al. (2011) In vivo kinetics of [F-18]MEFWAY: a comparison with [C-11]WAY100635 and [F-18]MPPF in the nonhuman primate. Synapse 65: 592-600.
4. Koba W, Jelicks LA, Fine EJ (2012) MicroPET/SPECT/CT Imaging of Small Animal Models of Disease. Am J Pathol 182: 319-324.
5. Rice O, Saintvictor S, Michaelides M, Thanos P, Gatley SJ (2006) MicroPET investigation of chronic long-term neurotoxicity from heavy ion irradiation. AAPS J 8: E508-E514
6. Zhang X, Paule MG, Newport GD, Liu F, Callicott R, et al. (2012) MicroPET/CT Imaging of [18F]-FEPPA in the Nonhuman Primate: A Potential Biomarker of Pathogenic Processes Associated with Anesthetic-Induced Neurotoxicity. ISRN Anesthesiology.
7. Zhang X, Paule MG, Newport GD, Sadovova N, Berridge MS, et al. (2011) MicroPET imaging of ketamine-induced neuronal apoptosis with radiolabeled DFNSH. J Neural Transm 118: 203-211.
8. Zhang X, Paule MG, Newport GD, Zou X, Sadovova N, et al. (2009) A minimally invasive, translational biomarker of ketamine-induced neuronal death in rats: microPET Imaging using 18F-annexin V. Toxicol Sci 111: 355-361.
9. Campbell LL, Tyson JA, Stackpole EE, Hokenson KE, Sherrill H, et al. (2011) Assessment of general anaesthetic cytotoxicity in murine cortical neurones in dissociated culture. Toxicology 283: 1-7.
10. Jevtovic-Todorovic V, Hartman RE, Izumi Y, Benshoff ND, Dikranian K, et al. (2003) Early exposure to common anesthetic agents causes widespread neurodegeneration in the developing rat brain and persistent learning deficits. J Neurosci 23: 876-882.
11. Wang S, Peretich K, Zhao Y, Liang G, Meng Q, et al. (2009) Anesthesia-induced neurodegeneration in fetal rat brains. Pediatr Res 66: 435-440.
12. Zou X, Sadovova N, Patterson TA, Divine RL, Hotchkiss CE, et al. (2008) The effects of L-carnitine on the combination of, inhalation anesthetic-induced developmental, neuronal apoptosis in the rat frontal cortex. Neuroscience 151: 1053-1065.
13. Paule MG, Li M, Allen RR, Liu F, Zou X, et al. (2011) Ketamine anesthesia during the first week of life can cause long-lasting cognitive deficits in rhesus monkeys. Neurotoxicol Teratol 33: 220-230.
14. Zou X, Liu F, Zhang X, Patterson TA, Callicott R, et al. (2011) Inhalation anesthetic-induced neuronal damage in the developing rhesus monkey. Neurotoxicol Teratol 33: 592-597.
15. Alves E, Binienda Z, Carvalho F, Alves CJ, Fernandes E, et al. (2009) Acetyl-L-carnitine provides effective in vivo neuroprotection over 3,4-methylenedioximethamphetamine-induced mitochondrial neurotoxicity in the adolescent rat brain. Neuroscience 158: 514-523.
16. Calabrese V, Cornelius C, Mancuso C, Pennisi G, Calafato S, et al. (2008) Cellular stress response: a novel target for chemoprevention and nutritional neuroprotection in aging, neurodegenerative disorders and longevity. Neurochem Res 33: 2444-2471.
17. Jones LL, McDonald DA, Borum PR (2010) Acylcarnitines: role in brain. Prog Lipid Res 49: 61-75.
18. McDaniel MA, Maier SF, Einstein GO (2003) "Brain-specific" nutrients: a memory cure? Nutrition 19: 957-975.
19. Abdul HM, Butterfield DA (2007) Involvement of PI3K/PKG/ERK1/2 signaling pathways in cortical neurons to trigger protection by cotreatment of acetyl-L-carnitine and alpha-lipoic acid against HNE-mediated oxidative stress and neurotoxicity: implications for Alzheimer's disease. Free Radic Biol Med 42: 371-384.
20. Abdul HM, Calabrese V, Calvani M, Butterfield DA (2006) Acetyl-L-carnitine-induced up-regulation of heat shock proteins protects cortical neurons against amyloid-beta peptide 1-42-mediated oxidative stress and neurotoxicity: implications for Alzheimer's disease. J Neurosci Res 84: 398-408.
21. Calabrese V, Giuffrida Stella AM, Calvani M, Butterfield DA (2006) Acetylcarnitine and cellular stress response: roles in nutritional redox homeostasis and regulation of longevity genes. J Nutr Biochem 17: 73-88.
22. Calabrese V, Ravagna A, Colombrita C, Scapagnini G, Guagliano E, et al. (2005) Acetylcarnitine induces heme oxygenase in rat astrocytes and protects against oxidative stress: involvement of the transcription factor Nrf2. J Neurosci Res 79: 509-521.
23. Ishii T, Shimpo Y, Matsuoka Y, Kinoshita K (2000) Anti-apoptotic effect of acetyl-l-carnitine and l-carnitine in primary cultured neurons. Jpn J Pharmacol 83: 119-124.

24. Virmani MA, Caso V, Spadoni A, Rossi S, Russo F, et al. (2001) The action of acetyl-L-carnitine on the neurotoxicity evoked by amyloid fragments and peroxide on primary rat cortical neurones. Ann N Y Acad Sci 939: 162-178.

25. Zaitone SA, Abo-Elmatty DM, Shaalan AA (2012) Acetyl-L-carnitine and α-lipoic acid affect rotenone-induced damage in nigral dopaminergic neurons of rat brain, implication for Parkinson's disease therapy. Pharmacol Biochem Behav 100: 347-360.

26. Zanelli SA, Solenski NJ, Rosenthal RE, Fiskum G (2005) Mechanisms of ischemic neuroprotection by acetyl-L-carnitine. Ann N Y Acad Sci 1053: 153-161.

27. Hotchkiss CE, Wang C, Slikker W Jr (2007) Effect of prolonged ketamine exposure on cardiovascular physiology in pregnant and infant rhesus monkeys (Macaca mulatta). J Am Assoc Lab Anim Sci 46: 21-28.

28. Slikker W Jr, Zou X, Hotchkiss CE, Divine RL, Sadovova N, et al. (2007) Ketamine-induced neuronal cell death in the perinatal rhesus monkey. Toxicol Sci 98: 145-158.

29. Wilson AA, Garcia A, Parkes J, McCormick P, Stephenson KA (2008) Radiosynthesis and initial evaluation of [18F]-FEPPA for PET imaging of peripheral benzodiazepine receptors. Nucl Med Biol 35: 305-314.

30. Berridge MS, Apana SM, Hersh J (2009) Teflon radiolysis as the major source of carrier in fluorine-18. J Label Compd Radiopharm 52: 543-548.

31. Hardwick M, Fertikh D, Culty M, Li H, Vidic B, et al. (1999) Peripheral-type benzodiazepine receptor (PBR) in human breast cancer: correlation of breast cancer cell aggressive phenotype with PBR expression, nuclear localization, and PBR-mediated cell proliferation and nuclear transport of cholesterol. Cancer Res 59: 831-842.

32. Oke BO, Suarez-Quian CA, Riond J, Ferrara P, Papadopoulos V (1992) Cell surface localization of the peripheral-type benzodiazepine receptor (PBR) in adrenal cortex. Mol Cell Endocrinol 87: R1-R6.

33. Olson JM, Ciliax BJ, Mancini WR, Young AB (1988) Presence of peripheral-type benzodiazepine binding sites on human erythrocyte membranes. Eur J Pharmacol 152: 47-53.

34. Venturini I, Zeneroli ML, Corsi L, Avallone R, Farina F, et al. (1998) Up-regulation of peripheral benzodiazepine receptor system in hepatocellular carcinoma. Life Sci 63: 1269-1280.

35. Imaizumi M, Briard E, Zoghbi SS, Gourley JP, Hong J, et al. (2008) Brain and whole-body imaging in nonhuman primates of [11C]PBR28, a promising PET radioligand for peripheral benzodiazepine receptors. Neuroimage 39: 1289-1298.

36. Lang S (2002) The role of peripheral benzodiazepine receptors (PBRs) in CNS pathophysiology. Curr Med Chem 9: 1411-1415.

37. Kuhlmann AC, Guilarte TR (1999) Regional and temporal expression of the peripheral benzodiazepine receptor in MPTP neurotoxicity. Toxicol Sci 48: 107-116.

38. Kuhlmann AC, Guilarte TR (2000) Cellular and subcellular localization of peripheral benzodiazepine receptors after trimethyltin neurotoxicity. J Neurochem 74: 1694-1704.

39. Bennacef I, Salinas C, Horvath G, Gunn R, Bonasera T, et al. (2008) Comparison of [11C]PBR28 and [18F]FEPPA as CNS peripheral benzodiazepine receptor PET ligands in the pig. J Nucl Med 49: 81.

40. Rusjan PM, Wilson AA, Bloomfield PM, Vitcu I, Meyer JH (2011) Quantitation of translocator protein binding in human brain with the novel radioligand [18F]-FEPPA and positron emission tomography. J Cereb Blood Flow Metab 31: 1807-1816.

41. Schweitzer PJ, Fallon BA, Mann JJ, Kumar JS (2010) PET tracers for the peripheral benzodiazepine receptor and uses thereof. Drug Discov Today 15: 933-942.

42. Binienda Z, Virmani A, Przybyla-Zawislak B, Schmued L (2004) Neuroprotective effect of L-carnitine in the 3-nitropropionic acid (3-NPA)-evoked neurotoxicity in rats. Neurosci Lett 367: 264-267.

43. Bresolin N, Freddo L, Vergani L, Angelini C (1982) Carnitine, carnitine acyltransferases, and rat brain function. Exp Neurol 78: 285-292.

44. Shug AL, Schmidt MJ, Golden GT, Fariello RG (1982) The distribution and role of carnitine in the mammalian brain. Life Sci 31: 2869-2874.

45. Virmani A, Binienda Z (2004) Role of carnitine esters in brain neuropathology. Mol Aspects Med 25: 533-549.

46. Virmani A, Gaetani F, Binienda Z (2005) Effects of metabolic modifiers such as carnitines, coenzyme Q10, and PUFAs against different forms of neurotoxic insults: metabolic inhibitors, MPTP, and methamphetamine. Ann N Y Acad Sci 1053: 183-191.

47. Rump TJ, Abdul Muneer PM, Szlachetka AM, Lamb A, Haorei C, et al. (2010) Acetyl-L-carnitine protects neuronal function from alcohol-induced oxidative damage in the brain. Free Radic Biol Med 49: 1494-1504.

48. Barhwal K, Hota SK, Prasad D, Singh SB, Ilavazhagan G (2008) Hypoxia-induced deactivation of NGF-mediated ERK1/2 signaling in hippocampal cells: neuroprotection by acetyl-L-carnitine. J Neurosci Res 86: 2705-2721.

49. Scafidi S, Racz J, Hazelton J, McKenna MC, Fiskum G (2010) Neuroprotection by acetyl-L-carnitine after traumatic injury to the immature rat brain. Dev Neurosci 32: 480-487.

50. De Angelis C, Scarfò C, Falcinelli M, Perna E, Reda E (1994) Acetyl-L-carnitine prevents age-dependent structural alterations in rat peripheral nerves and promotes regeneration following sciatic nerve injury in young and senescent rats. Exp Neurol 128: 103-114.

51. Manfridi A, Forloni GL, Arrigoni-Martelli E, Mancia M (1992) Culture of dorsal root ganglion neurons from aged rats: effects of acetyl-L-carnitine and NGF. Int J Dev Neurosci 10: 321-329.

52. Winter BK, Fiskum G, Gallo LL (1995) Effects of L-carnitine on serum triglyceride and cytokine levels in rat models of cachexia and septic shock. Br J Cancer 72: 1173-1179.

53. Zhang R, Zhang H, Zhang Z, Wang T, Niu J, et al. (2012) Neuroprotective Effects of Pre-Treament with l-Carnitine and Acetyl-l-Carnitine on Ischemic Injury In Vivo and In Vitro. Int J Mol Sci 13: 2078-2090.

54. Spagnoli A, Lucca U, Menasce G, Bandera L, Cizza G, et al. (1991) Long-term acetyl-L-carnitine treatment in Alzheimer's disease. Neurology 41: 1726-1732.